Langmuir-Blodgett Films of the Metal-Organic Framework MIL-101(Cr): Preparation, Characterization and CO$_2$ Adsorption Study Using a QCM-Based Setup

Javier Benito,[†,‡] Sara Sorribas,[§,‡] Irene Lucas,[Ω,‡] Joaquin Coronas,[§,‡] Ignacio Gascon[†,‡,*]

[†]Departamento de Química Física, Facultad de Ciencias, Universidad de Zaragoza, 50009 Zaragoza, Spain

[‡]Instituto de Nanociencia de Aragón (INA), Universidad de Zaragoza, 50018 Zaragoza, Spain

[§]Chemical and Environmental Engineering Department, Universidad de Zaragoza, 50018 Zaragoza, Spain

[Ω]Departamento de Física de la Materia Condensada, Facultad de Ciencias, Universidad de Zaragoza, 50009 Zaragoza, Spain.

CORRESPONDING AUTHOR

(I.G.) E-mail: igascon@unizar.es, phone number: +34 976761204.

ABSTRACT

This work reports the fabrication and characterization of Langmuir-Blodgett films of nanoparticles (size 51 ± 10 nm) of the metal organic framework MIL-101(Cr). LB film characterization by SEM, UV-vis, GIXRD and QCM has shown that the addition of 1 wt.% of behenic acid to MOF dispersion allows obtaining dense monolayers at the air-water interface that can be deposited onto solid substrates of different nature with transfer ratios close to 1. Moreover, a QCM-based setup has been built and used for the first time to measure CO_2 adsorption isotherms at 303 K on MOF LB films, proving that LB films with MOF masses between 1.2 (1 layer) and 2.3 (2 layers) micrograms can be used to obtain accurate adsorption values at 100 kPa, similar to those obtained by conventional adsorption methods that require much larger MOF quantities (tens of milligrams).

INTRODUCTION

Metal-organic frameworks[1] (MOFs) are hybrid materials with outstanding properties that make them promising candidates for a wide range of applications,[2-3] including gas storage[4] and membrane separation,[5] heterogeneous catalyst,[6] encapsulation[7] and drug delivery,[8] electronics,[9] etc. In particular, the integration of MOFs as functional materials into nanotechnological devices, such as chemical sensors, requires the deposition of MOF thin films onto solid supports.[10]

In recent years studies dealing with the fabrication of surface-mounted MOFs[10] (SURMOFs) have attracted increasing interest, and a large number of processes have been used to deposit MOF coatings onto solid substrates. Generally, the direct growth of MOF films by immersion of the solid support in the reaction mixture[11] produces films with thicknesses that range from some hundreds of nanometers to several micrometers. To fabricate thinner MOF films, strategies based on liquid phase epitaxy (LPE) are mainly used.[12] Among these methods, the most widespread is the successive immersion of the functionalized substrate in two different solutions that contain, respectively, the metal precursor and the organic ligand. This process is successively repeated and the final thickness of the film depends on the number of immersion cycles. In this method, gold supports functionalized with self-assembled monolayers (SAMs) of organic molecules are typically used.[13] In this context, different SURMOFs have been directly grown on SAM-modified quartz crystal microbalance (QCM) gold substrates and the adsorption and desorption of different substances onto the films have been monitored.[14] QCM substrates coated with SURMOFs are very interesting systems for the development of chemical sensors and also for studying and characterizing fundamental properties of MOFs such as mass transfer processes.[15]

Another interesting approach for the deposition of MOF thin films is the Langmuir-Blodgett (LB) technique that allows the fabrication at the air-liquid interface of monolayers of different kinds of materials including organic molecules, polymers or nanoparticles (NPs). These monolayers can be subsequently deposited onto substrates of different nature (glass, quartz, silicon, etc.) generally without any previous functionalization.[16] Also the total thickness of the LB films may be controlled by varying the number of deposition cycles, which makes the LB method an ideal tool to explore the implementation of MOFs into devices.

Surprisingly, the LB technique has scarcely been explored for MOF deposition. MOF crystals of micrometric size and different morphologies have been transferred by the LB method and their orientation characterized using XRD and SEM.[17] However, most of the existing studies combine the LB and the layer-by-layer method to obtain nanofilms of a family of MOFs named NAFS.[18-19] In a recent study we explored the fabrication of mixed LB films containing the MOF NH_2-MIL88B(Fe) and a commercial polyimide, showing that it is possible to obtain ultrathin MOF + polymer films with a homogeneous distribution of MOF particles on the polymer matrix.[20] Mixed MOF-polymer LB films are of great interest for the development of ultrathin MOF-based mixed matrix membranes.[21]

Following our exploration of the LB technique to obtain MOF thin films incorporated into different solid substrates, in this contribution MIL-101(Cr) NPs of size ca. 50 nm have been synthesized and LB films have been fabricated onto quartz, glass and silicon supports and characterized using UV-vis, SEM and GIXRD. Also a QCM-based setup has been built to study CO_2 adsorption on LB films transferred onto gold QCM substrates. As far as we know, there are no previous studies in the literature dealing with the deposition and characterization of MOF LB films onto QCM substrates.

MIL-101(Cr) is a well-known chromium terephthalate-based MOF that has a large surface area and high stability;[22] moreover it presents attractive properties for CO_2 capture[23] and membrane based applications.[24] In addition, its hydrophilic character may help to obtain homogenous monolayers at the air-water interface. Previous studies have shown that it is possible to obtain MIL-101(Cr) thin films by dip-coating silicon wafers in a colloidal solution of MIL-101(Cr) NPs (average size 22 ± 5 nm) prepared in ethanol.[25] Using the same solvent in the presence of the polymer polyethylenimine (PEI), a dip-coating method has been used to fabricate thin films of MIL-101(Cr) NPs (average size 50 nm) on alumina supports.[26] This study has shown that PEI improves the interaction of the MOF NPs with the surface of the alumina support while at the same time reducing the stress forces between the MOF NPs. Inspired by these results, behenic acid (BA), a well-known surfactant that forms stable Langmuir films,[27] has been used in the present study to reduce NP aggregation at the air-water interface.

MATERIALS AND METHODS

MOF synthesis and characterization: MIL-101(Cr) was synthesized according to a previously reported procedure[24] followed by some additional purification steps described in the literature.[28] Briefly: 0.7 g of chromium chloride hexahydrate ($CrCl_3 \cdot 6H_2O$, Sigma-Aldrich, $\geq$ 98 %) was mixed with 26 mL of deionized water. Then 0.45 g of terephthalic acid (H_2BDC, Sigma-Aldrich, 98 %) was added. The mixture was placed inside a PTFE-TFM pressure vessel, and then heated in a microwave oven (Multiwave 3000, Anton Paar) to 453 K for 30 min. The sample was recovered by centrifugation at 10000 rpm for 10 min and washed several times with deionized water. To remove the terephtalic acid remaining within the pores of the MOF, MIL-101(Cr) was dispersed in EtOH (1 g dispersed in 50 mL), placed in an autoclave and heated to

373 K overnight. After that, the product was recovered by centrifugation at 10000 rpm for 10 min and dispersed in an aqueous solution of NH_4F 30 mM (1 g dispersed in 150 mL) at 333 K for 10 h. Finally the solid was washed with abundant hot water to remove traces of NH_4F, dispersed in MeOH and stored in the solvent. No drying was applied to the material to minimize NP aggregation.

SEM images of the obtained NP powder were taken at 15 kV with a FEG column using a SEM INSPECT F50 (FEI Company). NP powder XRD analysis was made using a D-Max Rigaku X-ray diffractometer with a copper anode and a graphite monochromator (CuKα radiation, $\lambda = 1.5418$ Å).

The specific surface area of MIL-101(Cr) was calculated using a Micromeritics Tristar 3000 with N_2 at 77.4 K. Prior to the N_2 adsorption/desorption measurement the sample was degassed under vacuum for 8 h at 453 K. The specific surface area was calculated according to the BET (Brunauer-Emmett-Teller) method. CO_2 adsorption/desorption isotherms were measured with Micromeritics ASAP 2020 equipment at 303 K using water as a coolant.

Langmuir and Langmuir-Blodgett film fabrication and characterization: Surface pressure-area (π-A) and surface potential-area (ΔV-A) isotherms were obtained simultaneously using a Teflon made Langmuir trough NIMA model 702, (dimensions 720 mm×100 mm). Another apparatus was used to obtain Langmuir-Blodgett films. This was a KSV-NIMA trough model KN 2003, with dimensions of 580 mm×145 mm. In both cases, compression was performed by a symmetric double-barrier system at constant speed, 6 $cm^2 \cdot min^{-1}$. These troughs were kept in a clean room inside closed cabinets and the temperature was maintained at 293 K (± 1 K). Ultra-Pure Milli-Q water

(ρ = 18.2 MΩ·cm) was employed as a subphase in all the experiments. A KSV Potential Sensor was used to obtain surface potential measurements.

Chloroform (Panreac, > 99.9%) and methanol (Sigma-Aldrich, > 99.9%) were used to prepare 0.2 mg·mL^{-1} MIL-101(Cr) suspensions from the mother dispersion. Various proportions in the solvent mixture (4:1, 1:1 and 1:2 in volume of chloroform:methanol) were studied. The appropriate volume of behenic acid (BA), previously dissolved in chloroform (concentration 1·10^{-4} M), was added to the dispersion to obtain the desired mass percentages of MOF:BA. All the suspensions were stirred for 24 h to ensure homogeneity and sonicated during 5 min before film fabrication.

SEM images of the LB films deposited onto glass substrates were taken using the same SEM INSPECT F50 mentioned above. UV-Vis spectra of the LB films deposited onto quartz substrates were obtained using a Varian Cary 50 spectrophotometer with a normal incident angle with respect to the film plane. Grazing incidence X-ray diffraction (GIXRD) characterization of the films deposited onto Si(100) wafers was performed in a high resolution Empyrean diffractomer from PANalytical operating at 40kV and 40mA (CuKα radiation). This apparatus is equipped with a Pixcell 1D medipix3 detector and the scans were collected in the open detector mode. The grazing incidence angle (between 0.13º and 0.17º) was optimized for each sample before scan acquisition.

QCM-based setup for gas adsorption studies: A home-made QCM-based setup represented in Scheme 1 was built to perform gas adsorption studies. In this apparatus, measurements at temperatures up to 363 K and pressures up to 1.5 bar can be obtained. The setup consists of a stainless-steel chamber with a capacity of about 200 mL. Two QCM crystals of a resonant frequency of 9 MHz purchased from Inficon were placed

inside the chamber mounted onto two CHC-15 Crystal Holders (Inficon). One of the crystals was uncoated and used as a reference to correct possible fluctuations in the measurement due to temperature, pressure or gas flow.[29] The other crystal was coated with the material under study. Each holder was connected through a 2' cable SMB– SMB plug to an Inficon RQCM system with two Phase Lock Oscillators (PLOs) capable of working in a range of 5.1 to 10 MHz.

A total gas flow of 50 mL(STP)·min^{-1} was used in all the measurements. He (diluting gas) and CO_2 flows were controlled separately by two Alicat Scientific MC-100SCCM-D/5M mass-flow controllers. The pressure inside the chamber was monitored by means of a pressure sensor. Two temperature sensors allowed measuring the temperature inside the chamber, which was adjusted by two electric resistors. Before starting each measurement the sample was kept at a temperature of 343 K during 1 h under a constant flow of 50 mL(STP)·min^{-1} of He and then cooled to 303 K maintaining the He flow until a stable frequency was obtained. Adsorption measurements were done at constant temperature (303 K) using 5 different partial pressures of CO_2 in the mixture (CO_2 content was varied following the sequence: 20, 40, 60, 80 and 100% in volume). The frequency was allowed to stabilize before changing the gas mixture composition. At the end of the measurement, CO_2 was swept with pure He to observe the recovery of the samples.

RESULTS AND DISCUSSION

MOF characterization: SEM images demonstrate that nearly spherical MIL-101(Cr) nanocrystals of size 51 ± 10 nm were synthesized (see Figure 1.) The BET specific surface area of this material was 2300 $m^2 \cdot g^{-1}$. Also XRD of the NP powder was similar to previous studies.[24]

Langmuir and LB films: Langmuir films of MIL-101(Cr) were obtained at the air-water interface spreading 2 mL of MOF NP suspensions (0.2 $mg \cdot mL^{-1}$) prepared in different chloroform:methanol mixtures in order to find the best composition to optimize film homogeneity and reduce particle aggregation. For all the studied mixtures, Brewster Angle Microscopy (BAM) images (see Figure S1 of the supporting information) obtained during the compression of the films showed NP dense domains and uncovered water areas from the beginning of the compression. The formation of compact films that totally covered the water surface was observed at surface pressures above 5 $mN \cdot m^{-1}$.

Figure 2 shows the π-A and ΔV-A isotherms obtained during the compression of the film after spreading a suspension of MOF NPs prepared in chloroform:methanol in the proportion 4:1. The area is expressed in cm^2 of water surface available per mg of MOF spread.

π-A and ΔV-A isotherms are consistent with the formation of a compact film at the air-water interface. The surface pressure is almost zero over large areas and starts to increase at ca. 300 $cm^2 \cdot mg^{-1}$ of MOF. Upon further area reduction, π considerably rises, reaching values above 40 $mN \cdot m^{-1}$. The surface potential continuously increases from the beginning of the compression although some oscillations over large areas reveal the existence of uncovered water surface areas observed in BAM images. Two slope

growths at ca. 455 and 349 cm^2/mg of MOF precede the onset observed in the π-A isotherm before the surface potential reaches a value of ca. 256 mV at 285 cm^2/mg. From this point, ΔV increase less markedly until a new slope change takes place again at around 180 cm^2/mg of MOF, which is interpreted as the formation of 3D aggregates since a dense monolayer is already formed at lower areas according to the BAM images. Langmuir films obtained with all the chloroform:methanol mixtures analyzed were transferred onto glass substrates during substrate emersion at constant surface pressure (12 mN·m^{-1}) and characterized by SEM. Figure 3 shows that the obtained LB films (1 layer) were reasonably compact although more defects could be observed in the film when a mixture in the proportion 4:1 was used. Also particle aggregation was increased for that mixture. The more homogeneous and compact LB monolayers were obtained for the mixture in the volume proportion 1:1. Although these results proved that methanol reduced particle aggregation, there were some issues with the reproducibility of the π-A and ΔV-A isotherms when the content of methanol in the mixtures was larger than 20% in volume, probably due to a partial dispersion of MOF NPs into the aqueous subphase.

To avoid the loss of material and to improve the homogeneity of the films, BA was added to MOF suspensions prepared in chloroform:methanol (4:1). Different amounts of BA were tested, concluding that just 1 % in mass of BA (relative to the MOF mass in the dispersion) was enough to produce a reproducible expansion in the area per mass of MOF at a given surface pressure. π-A and ΔV-A isotherms obtained when 1% of BA was added to MOF NPs are compared with those of the MOF NPs in Figure 2. As can be observed, the expansion in the π-A isotherm was significant (area per mg of MOF increases around 20%) but surface potential values scarcely changed. This expansion was interpreted as a reduction of NP aggregation at the air-water interface and an

increment of the amount of NPs in contact with the water surface. To prove this hypothesis, LB films were transferred at 12 mN·m^{-1} during the upstroke of glass substrates and characterized by SEM (Figure 4).

A comparison between LB films (1 layer) obtained with and without BA in the NP dispersions confirms that BA reduces defects in the films and particle aggregation, allowing the formation of MOF NP dense monolayers that can be incorporated into substrates of different nature to cover large areas.

To complete the characterization of the samples, LB films prepared under the same experimental conditions (surface pressure 12 mN·m^{-1}, solution containing 1% in mass of BA) were deposited onto quartz slides and Si(100) wafers for UV and GIXRD characterization.

The UV spectrum of the LB film (1 layer) showed a well-defined intense absorption peak at 250 nm (Figure 5). Moreover, when a new film was transferred onto the same substrate, the absorbance was doubled, proving that the density of the second layer was similar to that of the film in contact with the quartz substrate.

Figure 6 shows the GIXRD patterns of LB (3 layers) and drop-cast films deposited onto Si(100) wafers. The XRD of the NP powder and the simulated XRD obtained from the crystallographic structure information reported for this material[30] are also plotted in the same figure for the purposes of comparison. As can be observed, XRD pattern of the NP powder shows the characteristic diffraction peaks of MIL-101(Cr) with broader Bragg reflections, in agreement with the presence of small NPs.[25-26] The GIXRD patterns of the films (cast and LB) present similar characteristics to the powder XRD, which seems to indicate that the crystallinity of the material was not affected during film fabrication, although some of the diffraction peaks are less marked probably due to the small amount of material deposited in the samples. This effect is more noticeable in the LB

films, especially when only 1 layer is deposited (see Figure S2 of the supporting information). Similarly, the GI-WAXS pattern reported for a thin film of MIL-101(Cr) NP prepared by dip-coating[25] showed very similar characteristics to the LB films, with less defined peaks than the powder material.

CO2 adsorption studies using QCM-based setup: CO_2 adsorption studies were performed with the QCM-based setup at 303 K (pressure 100 kPa) following the procedure described in section 2.3. LB films (one or two layers deposited) and drop-cast films prepared using NP diluted suspensions, some containing BA and others not, were studied for comparison. At least three different samples of each type were analyzed and the average values and standard deviations obtained in these studies are summarized in Table 1. Moreover, average adsorption data obtained from QCM experiments have been represented in Figure 7. Error bars in this figure are standard deviations of the measurements (error bar in some points are almost not visible due to the size of the symbols).

Following a reported methodology,[29] the accuracy of the setup was tested comparing the amount of CO_2 adsorbed on MIL-101(Cr) NP powder determined by a conventional analytical method (Micromeritics ASAP 2020 equipment) and the CO_2 adsorption on drop-cast films prepared using NP suspensions (without BA) obtained by QCM frequency change measurements. The average values obtained using both methods were analogous, as can be observed in Figure 7, confirming that the setup as built could be used to obtain accurate adsorption data using small amounts of material (a few micrograms versus several tens of milligrams in case of the conventional adsorption methodology). Previous studies also showed that QCM experiments performed with

drop-cast films (deposited MOF mass 3-7 μg) could be used to study the kinetics of the desorption processes of guest molecules from the pores of different MOFs.[31]

LB films obtained at the best working conditions tested (MIL-101(Cr) + 1% BA) were then deposited onto QCM substrates at 12 mN·m^{-1} for CO_2 adsorption studies. The change in the resonant frequency after the deposition of the film was first used to determine the mass of MOF deposited using the Sauerbrey equation,[32] $\Delta f = - C_f \cdot \Delta m$, where Δf is the observed frequency change in Hz, C_f is the sensitivity factor of the QCM crystal (0.1834 Hz·ng^{-1}·cm^2) provided by Inficon and Δm is the change in mass per unit area. The obtained mass of MOF deposited in one transference was ca. 1.2 μg. Taking into account that the active oscillation region of the QCM substrate is 34.2 mm^2, this gives 3.5 μg·cm^{-2}, which is in good agreement with the observed area per mass of MOF at the surface pressure of transference (3.8 μg·cm^{-2}) giving a transfer ratio close to 1 (0.92). Moreover, the deposition of a second layer almost doubled the amount of MOF deposited.

As can be observed in Table 1, CO_2 adsorption was similar in all the samples (cast films, LB films with 1 or 2 layers) containing MIL-101(Cr) + 1% BA. In addition, Figure 7 shows the comparison between the CO_2 adsorption isotherms measured on LB film (2 layers) and cast film MIL-101(Cr) + 1% BA, showing that the behavior of the samples was almost identical. These results prove that using the LB technique it is possible to obtain compact NP MOF thin films that can be directly deposited onto QCM substrates to study adsorption processes using a minimal amount of material. Moreover, the time needed to fabricate one LB film is ca. 3 h, which is significantly shorter than the time required for SURMOF fabrication using the LPE methodology, where 72 h are needed to grow a film of 100 nm of HKUST-1.[33] This opens up a very interesting

methodology for the development of new tools for both MOF characterization and chemical sensors.

MIL-101(Cr) + 1% BA samples exhibited lower CO_2 adsorption than MIL-101(Cr), probably due to partial BA penetration into the MOF pores. A similar reduction in adsorption has been reported when PEI was used to prepare MIL-101(Cr) thin films on alumina supports.[26] However, it should be emphasized that BA was necessary to obtain dense MOF films on QCM substrates. When MIL-101(Cr) Langmuir films prepared without BA were directly transferred onto QCM substrates, poor coverage of the substrates was obtained (transfer ratio below 0.4).

Figure S3 of the supporting information shows the resonant frequency change of a QCM substrate covered with a LB film (2 layers) during CO_2 adsorption measurements. Less than 60 min were necessary to obtain the five experimental points. Additionally, in the same figure, the effect of using He at the end of the experiment to remove the adsorbed CO_2 can be observed. About 15 min of He flow at 303 K were enough to obtain a resonant frequency that was almost the same as the initial value of the experiment, showing that the adsorption process was reversible (heating at 343 K the sample was completely recovered).

CONCLUSIONS

The formation of ultrathin films of the metal organic framework MIL-101(Cr) at the air-water interface has been studied, showing that the optimization of the solvent proportion and the addition of a small amount of BA (1% of MOF mass) to MOF NP (size 51 ± 10 nm) dispersions allows obtaining compact and dense monolayers that can be transferred onto solid substrates of different nature (glass, quartz, silicon). SEM, UV-vis and GIXRD characterization has confirmed the compact packing of MOF NPs. Moreover,

for the first time MOF NP LB films have been incorporated into QCM substrates by direct transfer from the air-water interface without any previous substrate functionalization. The obtained LB films have been studied at 303 K for CO_2 adsorption, measuring resonant frequency changes during gas flow at 5 different CO_2 partial pressures. The total amount of CO_2 adsorbed at 100 kPa can be characterized using QCM substrates modified with just one LB layer. The amount of MOF deposited in one transfer (1.2 g) is enough to obtain accurate adsorption values, comparable to those obtained by conventional adsorption methods that require much larger MOF quantities (tens of mg). These results open up an interesting approach for the preparation and characterization of MOF thin films and their use in the development of new characterization tools and chemical sensors.

ASSOCIATED CONTENT

Figures showing BAM images of Langmuir film formation, GIXRD characterization of LB films (1 and 3 layers) and the resonant frequency change of a QCM during a CO_2 adsorption experiment. This material is available free of charge via the Internet at http://pubs.acs.org

REFERENCES

(1)   Li, H.; Eddaoudi, M.; O'Keeffe, M.; Yaghi, O. M., Design and Synthesis of an Exceptionally Stable and Highly Porous Metal-Organic Framework. *Nature* **1999**, *402* (6759), 276-279.

(2)   Kitagawa, S.; Kitaura, R.; Noro, S., Functional Porous Coordination Polymers. *Angew. Chem., Int. Ed.* **2004**, *43* (18), 2334-2375.

(3)   Ferey, G., Hybrid Porous Solids: Past, Present, Future. *Chem. Soc. Rev.* **2008**, *37* (1), 191-214.

(4)   Fracaroli, A. M.; Furukawa, H.; Suzuki, M.; Dodd, M.; Okajima, S.; Gandara, F.; Reimer, J. A.; Yaghi, O. M., Metal-Organic Frameworks with Precisely Designed Interior for Carbon Dioxide Capture in the Presence of Water. *J. Am. Chem. Soc.* **2014**, *136* (25), 8863-8866.

(5)   Yeo, Z. Y.; Chai, S. P.; Zhu, P. W.; Mohamed, A. R., An Overview: Synthesis of Thin Films/Membranes of Metal Organic Frameworks and Its Gas Separation Performances. *RSC Adv.* **2014**, *4* (97), 54322-54334.

(6)   Rasero-Almansa, A. M.; Corma, A.; Iglesias, M.; Sanchez, F., Design of a Bifunctional Ir-Zr Based Metal-Organic Framework Heterogeneous Catalyst for the N-Alkylation of Amines with Alcohols. *Chemcatchem* **2014**, *6* (6), 1794-1800.

(7)   Paseta, L.; Potier, G.; Abbott, S.; Coronas, J., Using Hansen Solubility Parameters to Study the Encapsulation of Caffeine in MOFS. *Org. Biomol. Chem.* **2015**, *13* (6), 1724-1731.

(8)   Horcajada, P.; Chalati, T.; Serre, C.; Gillet, B.; Sebrie, C.; Baati, T.; Eubank, J. F.; Heurtaux, D.; Clayette, P.; Kreuz, C.; Chang, J. S.; Hwang, Y. K.; Marsaud, V.; Bories, P. N.; Cynober, L.; Gil, S.; Ferey, G.; Couvreur, P.; Gref, R., Porous Metal-Organic-Framework Nanoscale Carriers as a Potential Platform for Drug Delivery and Imaging. *Nat. Mater.* **2010**, *9* (2), 172-178.

(9)   Stavila, V.; Talin, A. A.; Allendorf, M. D., MOF-Based Electronic and Optoelectronic Devices. *Chem. Soc. Rev.* **2014**, *43* (16), 5994-6010.

(10)   Betard, A.; Fischer, R. A., Metal-Organic Framework Thin Films: From Fundamentals to Applications. *Chem. Rev.* **2012**, *112* (2), 1055-1083.

(11)   Zacher, D.; Baunemann, A.; Hermes, S.; Fischer, R. A., Deposition of Microcrystalline $[Cu_3(Btc)_2]$ and $[Zn_2(Bdc)_2(dabco)]$ at Alumina and Silica Surfaces Modified with Patterned Self Assembled Organic Monolayers: Evidence of Surface Selective and Oriented Growth. *J. Mater. Chem.* **2007**, *17* (27), 2785-2792.

(12)   Shekhah, O.; Wang, H.; Kowarik, S.; Schreiber, F.; Paulus, M.; Tolan, M.; Sternemann, C.; Evers, F.; Zacher, D.; Fischer, R. A.; Woll, C., Step-by-Step Route for the Synthesis of Metal-Organic Frameworks. *J. Am. Chem. Soc.* **2007**, *129* (49), 15118-15119.

(13)   Shekhah, O.; Wang, H.; Zacher, D.; Fischer, R. A.; Woll, C., Growth Mechanism of Metal-Organic Frameworks: Insights into the Nucleation by Employing a Step-by-Step Route. *Angew. Chem., Int. Ed.* **2009**, *48* (27), 5038-5041.

(14)   Betard, A.; Wannapaiboon, S.; Fischer, R. A., Assessing the Adsorption Selectivity of Linker Functionalized, Moisture-Stable Metal-Organic Framework Thin

Films by Means of an Environment-Controlled Quartz Crystal Microbalance. *Chem. Commun.* **2012**, *48* (85), 10493-10495.

(15)　Heinke, L.; Gu, Z. G.; Woll, C., The Surface Barrier Phenomenon at the Loading of Metal-Organic Frameworks. *Nat. Commun.* **2014**, *5* (4562).

(16)　Ariga, K.; Yamauchi, Y.; Mori, T.; Hill, J. P., 25th Anniversary Article: What Can Be Done with the Langmuir-Blodgett Method? Recent Developments and its Critical Role in Materials Science. *Adv. Mater. (Weinheim, Ger.)* **2013**, *25* (45), 6477-6512.

(17)　Tsotsalas, M.; Umemura, A.; Kim, F.; Sakata, Y.; Reboul, J.; Kitagawa, S.; Furukawa, S., Crystal Morphology-Directed Framework Orientation in Porous Coordination Polymer Films and Freestanding Membranes via Langmuir-Blodgettry. *J. Mater. Chem.* **2012**, *22* (20), 10159-10165.

(18)　Makiura, R.; Motoyama, S.; Umemura, Y.; Yamanaka, H.; Sakata, O.; Kitagawa, H., Surface Nano-Architecture of a Metal-Organic Framework. *Nat. Mater.* **2010**, *9* (7), 565-571.

(19)　Makiura, R.; Kitagawa, H., Porous Porphyrin Nanoarchitectures on Surfaces. *Eur. J. Inorg. Chem.* **2010**, (24), 3715-3724.

(20)　Benito, J.; Fenero, M.; Sorribas, S.; Zornoza, B.; Msayib, K. J.; McKeown, N. B.; Téllez, C.; Coronas, J.; Gascón, I., Fabrication of Ultrathin Films Containing the Metal Organic Framework Fe-MIL-88B-NH$_2$ by the Langmuir–Blodgett Technique. *Colloids Surf., A* **2015**, *470* (0), 161-170.

(21)　Seoane, B.; Coronas, J.; Gascon, I.; Benavides, M. E.; Karvan, O.; Caro, J.; Kapteijn, F.; Gascon, J., Metal-Organic Framework Based Mixed Matrix Membranes: A Solution for Highly Efficient CO$_2$ Capture? *Chem. Soc. Rev.* **2015**, *44* (8), 2421-2454.

(22)   Ferey, G.; Mellot-Draznieks, C.; Serre, C.; Millange, F.; Dutour, J.; Surble, S.; Margiolaki, I., A Chromium Terephthalate-Based Solid with Unusually Large Pore Volumes and Surface Area. *Science* **2005**, *309* (5743), 2040-2042.

(23)   Liu, Q.; Ning, L. Q.; Zheng, S. D.; Tao, M. N.; Shi, Y.; He, Y., Adsorption of Carbon Dioxide by MIL-101(Cr): Regeneration Conditions and Influence of Flue Gas Contaminants. *Sci. Rep.* **2013**, *3*.

(24)   Sorribas, S.; Gorgojo, P.; Tellez, C.; Coronas, J.; Livingston, A. G., High Flux Thin Film Nanocomposite Membranes Based on Metal-Organic Frameworks for Organic Solvent Nanofiltration. *J. Am. Chem. Soc.* **2013**, *135* (40), 15201-15208.

(25)   Demessence, A.; Horcajada, P.; Serre, C.; Boissiere, C.; Grosso, D.; Sanchez, C.; Ferey, G., Elaboration and Properties of Hierarchically Structured Optical Thin Films of MIL-101(Cr). *Chem. Commun.* **2009**, (46), 7149-7151.

(26)   Jiang, D. M.; Burrows, A. D.; Xiong, Y. L.; Edler, K. J., Facile Synthesis of Crack-Free Metal-Organic Framework Films on Alumina by a Dip-Coating Route in the Presence of Polyethylenimine. *J. Mater. Chem. A* **2013**, *1* (18), 5497-5500.

(27)   Gaines, G. L., *Insoluble Monolayers at Liquid-Gas Interface*. Interscience Publisers. John Wiley & Sons: New York, **1966**.

(28)   Llewellyn, P. L.; Bourrelly, S.; Serre, C.; Vimont, A.; Daturi, M.; Hamon, L.; De Weireld, G.; Chang, J. S.; Hong, D. Y.; Hwang, Y. K.; Jhung, S. H.; Ferey, G., High Uptakes of CO_2 and CH_4 in Mesoporous Metal-Organic Frameworks MIL-100 and MIL-101. *Langmuir* **2008**, *24* (14), 7245-7250.

(29)   Venkatasubramanian, A.; Navaei, M.; Bagnall, K. R.; McCarley, K. C.; Nair, S.; Hesketh, P. J., Gas Adsorption Characteristics of Metal–Organic Frameworks via Quartz Crystal Microbalance Techniques. *J. Phys. Chem. C* **2012**, *116* (29), 15313-15321.

(30)   Lebedev, O. I.; Millange, F.; Serre, C.; Van Tendeloo, G.; Ferey, G., First Direct Imaging of Giant Pores of the Metal-Organic Framework MIL-101. *Chem. Mater.* **2005**, *17* (26), 6525-6527.

(31)   Tsotsalas, M.; Hejcik, P.; Sumida, K.; Kalay, Z.; Furukawa, S.; Kitagawa, S., Impact of Molecular Clustering inside Nanopores on Desorption Processes. *J. Am. Chem. Soc.* **2013**, *135* (12), 4608-4611.

(32)   Sauerbrey, G., Verwendung Von Schwingquarzen Zur Wagung Dunner Schichten Und Zur Mikrowagung. *Z. Phys.* **1959**, *155* (2), 206-222.

(33)   Zhuang, J. L.; Terfort, A.; Woll, C., Formation of Oriented and Patterned Films of Metal-Organic Frameworks by Liquid Phase Epitaxy: A Review. *Coordin. Chem. Rev.* **2016**, *307*, 391-424.
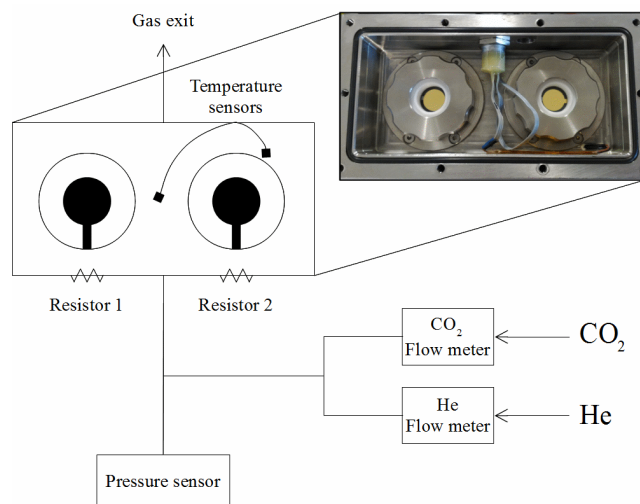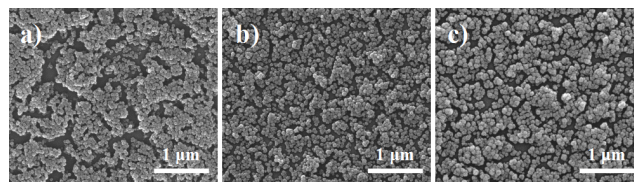
Scheme 1. Scheme of the QCM-based device used in CO_2 adsorption studies.
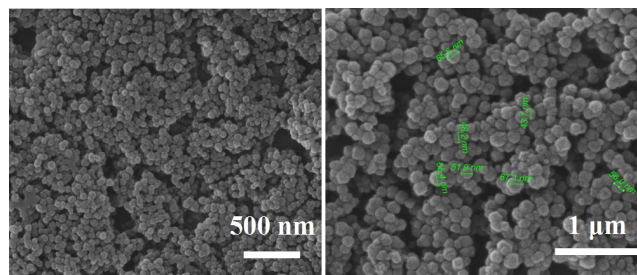
**Figure 1.** SEM images of as-synthesized MIL-101(Cr) nanocrystals.
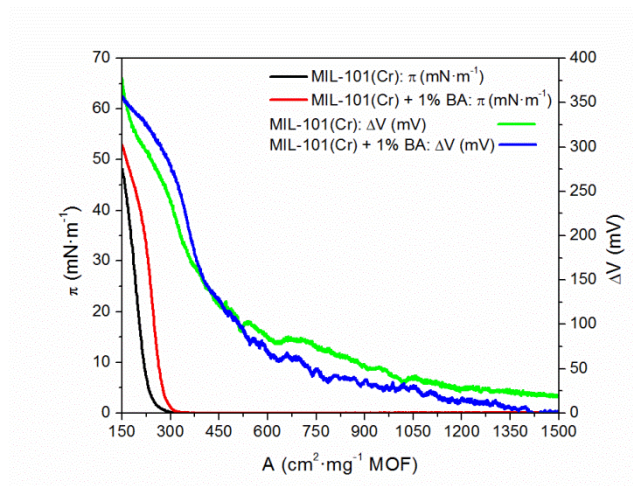
Figure 2. Surface pressure-area (π–A) and surface potential-area (ΔV-A) isotherms obtained using MOF NP dispersions in chloroform:methanol (4:1). MOF and MOF + 1% BA isotherms are plotted together for the purposes of comparison.
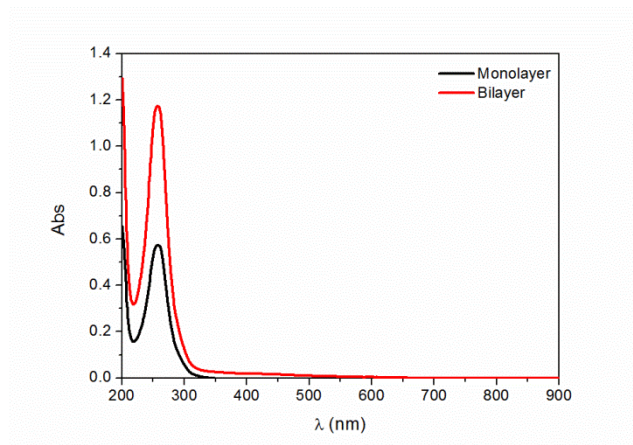
Figure 3. SEM images of LB films (1 layer) transferred at 12 mN·m^{-1} onto glass substrates using different chloroform:methanol mixtures to disperse MOF NP: a) 4:1 mixture b) 1:1 mixture c) 1:2 mixture.
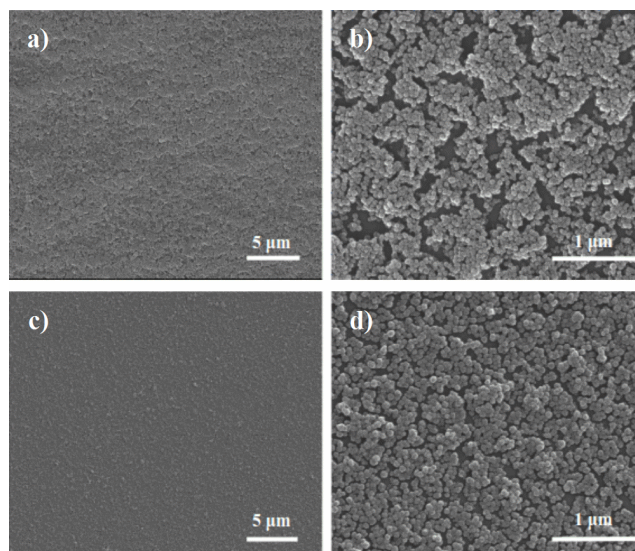
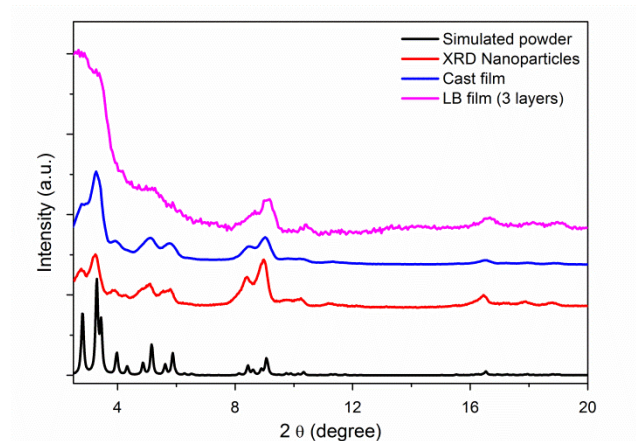**Figure 4.** SEM images of LB films (1 layer) transferred at 12 mN·m^{-1} onto glass substrates using MOF NP dispersions in chloroform:methanol (4:1). MOF film (a and b); MOF + 1% BA film (c and d).

Figure 5. UV spectra of LB films (MIL-101(Cr) + 1% BA) transferred at 12 mN·m^{-1} onto a quartz slide: 1 layer (black line), 2 layers (red line).

Figure 6. GIXRD patterns of MIL-101(Cr) + 1% BA drop-cast deposited sample (blue line) and three layer LB film (magenta line). For comparison, XRD of the NP powder MIL-101(Cr) (red line) and simulated XRD of the crystalline material (black line) have also been included.
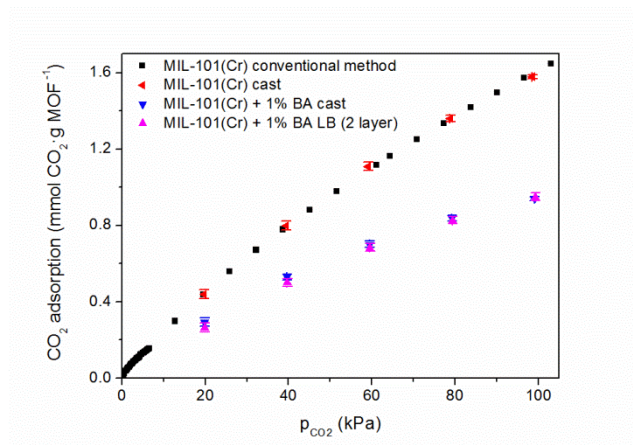
Figure 7. Average CO_2 adsorption values at 303 K obtained for MIL-101(Cr) samples using the QCM-based setup: MIL-101(Cr) cast film (◀), MIL-101(Cr) + 1% BA cast film (▼), MIL-101(Cr) + 1% BA LB (2 layers) film (▲). Error bars are standard deviations obtained from the analysis of at least three samples. MOF NP powder adsorption isotherm obtained by a conventional analytical method (■) is also shown for comparison.

Sample	Average MOF mass (μg)	CO_2 adsorption (mmol of CO_2/g of MOF)
Cast-film (MOF)	5.6	1.58 ± 0.01
Cast-film (MOF + 1% BA)	5.4	0.94 ± 0.01
LB film (MOF + 1% BA, 2 layers)	2.3	0.94 ± 0.02
LB film (MOF + 1% BA, 1 layer)	1.2	0.90 ± 0.05

Table 1. Amount of CO_2 adsorbed per mass of MOF (average ± standard deviation) at 303 K (CO_2 pressure 100 kPa) calculated using resonant frequency change in drop-cast and LB samples.